

2017 Connaught Summer Institute in Arctic Science

Poster Session Winners

MSc Winner (1)

Winner

Laurence Coursol

(UQAM)

Impact of far infrared measurements on analyses of temperature and humidity

Optimal configuration of a far infrared radiometer based on information content
Laurence Coursol, Q. Libois, L. S. Pelletier, P. Gauthier, J-P. Blanchet
Department of Earth and Atmospheric Sciences, University of Québec in Montreal, Montréal, Canada.

Introduction

Data assimilation optimally combines numerical weather predictions (NWP) and huge amounts of observations to provide the best weather analysis and forecast. In this context, a large part of the observations comes from satellite radiances particularly in the mid-infrared (M-IR), by sensors such as AIRS and IASI. However, the M-IR constitutes only half of the Earth's emitted radiance, the other half being the far infrared (F-IR), ranging from 45 to 100 μm . Recently, a number of theoretical studies have shown the added-value of F-IR observations for remote sensing of water vapor and clouds, especially in dry and cold regions. This study shows the added-value of F-IR radiometry with the future satellite TICFIRE (Thin Ice Clouds in Far IR Experiment) in polar regions compared to M-IR measurements with AIRS. To do so, the analysis error, i.e. error on the atmospheric profile after assimilating data, will be compared to the background error to quantify the information gained by observations in the F-IR and M-IR.

Advantage of F-IR measurements

- M-IR and F-IR both contain water vapor bands
- Atmospheric profiling of water vapor possible with the 6.3 μm band and the 15- 90 μm band
- Spectral resolution of the instruments:
 - AIRS $\approx 0.01 \mu\text{m}$
 - TICFIRE $\approx 1 \mu\text{m}$

Objectives

To determine the added-value of assimilating F-IR radiances in NWP systems

- Quantify the added information brought in by F-IR measurements when added to those in the M-IR in polar regions.
- Find an optimal configuration for a radiometer (3 to 100 μm)

Theory

• Data assimilation

$$\mathbf{x}_a = \mathbf{x}_b + \mathbf{K}(\mathbf{y} - \mathbf{H}\mathbf{x}_b)$$

Where $\mathbf{K} = \mathbf{B}\mathbf{H}^T(\mathbf{R} + \mathbf{H}\mathbf{B}\mathbf{H}^T)^{-1}$ is the gain matrix which gives a statistical weight to measurements and observations
 $\mathbf{H} = \frac{\partial \mathbf{R}(\mathbf{x})}{\partial \mathbf{x}} \Big|_{\mathbf{x}_b}$ is the Jacobian which gives the sensitivity of TOA radiance to small changes in atmospheric properties where $\mathbf{R}(\mathbf{x})$ is the radiative transfer model MODTRAN 5.4

- The 48 Jacobians were obtained by finite difference takes around a background state (T, ln q, ps, Ts)
- The background state is obtained from radiosonde profiles at 8 stations.

• Degrees of freedom per signal (DFS)
 $\text{DFS} = \text{tr}(\mathbf{H}\mathbf{K}) = \text{tr}(\mathbf{H}\mathbf{B}\mathbf{H}^T(\mathbf{H}\mathbf{B}\mathbf{H}^T + \mathbf{R})^{-1})$

- Allows to quantify the added-value of a set of observations
- Evaluation based on the relative errors between the observations and the prior information

References

- Bergman, C. W. D. Inverse methods for atmospheric sensing. Theory and practice. Vol. 2. World Scientific, 2000.
- Chouh, L., L. S. Pelletier, and M. P. Hertz. "Information error covariance associated with AIRS radiances observations: Influence and impact on data assimilation." *Journal of applied meteorology and climatology* 46 (2007): 754-755.
- Hertz, M. et al. "The far infrared bands." *Review of Geophysics* 45 (2007).
- Stachel, M., and J. P. Blanchet. "Improving observations (IS2) with an airborne spectrometer." *Journal of Atmospheric and Oceanic Technology* 31 (2014): 1360-1375.

Optimal configuration of the FIR instrument

- Optimal configuration is 50 bands DFS = 1.53
- 95% of the information with 4 bands of 50 bands
- Vertical lines gives the optimal bands for a constraint on the number of bands

- First two bands selected are 7 and 67 μm
- Bands are selected after from 50 to 20 μm
- Last band selected is 10 μm

FIRR and AIRS

- FIRR measurements reduces the error between 800 and 300 hPa
- Adding the measurements of FIRR over AIRS reduces the analysis error around 300 hPa

Optimized radiometer and AIRS

- Optimized FIRR is better at reducing the analysis error at 500 hPa
- No added-value to observations near the surface for the optimized FIRR.

Analysis error for humidity

Conclusions


- Measuring the added value of an instrument needs to be done with respect to what has already been gained from existing instruments
- The DFS (ratio of analysis error variance and background error variance) has been used to
 - Measure the added value of radiance measurements in the far infrared when assimilated on top of existing IR sounders
 - Examine different scenarios through OSSIA to optimize the configuration of the instrument
- Results show that measurements in the far infrared are over broader bands which increases the SNR and results in more accurate measurements.
- In cold situations, the FIR measurements bring a significant improvement to the vertical structure of the analysis

PhD Winners (2)

Winner Stephen McNamara

(U Michigan)


Nitrogen Oxide- Influenced Chlorine Chemistry in Utqiagvik (Barrow), Alaska



Contact:
smcnam@umich.edu

Nitrogen Oxide-Influenced Chlorine Chemistry in Utqiagvik (Barrow), Alaska

Stephen M. McNamara¹, Angela R. W. Raso^{1,2}, Siyuan Wang¹, Sham Thanekar³, Jose D. Fuentes¹, Paul B. Shepson^{2,4}, Kerri A. Pratt^{1,5}
¹Dept. of Chemistry, University of Michigan; ²Dept. of Chemistry, Purdue University; ³Dept. of Meteorology, Penn State University; ⁴Dept. of Earth, Atmospheric, and Planetary Sciences & Purdue Climate Change Research Center, Purdue University; ⁵Dept. of Earth and Environmental Sciences, University of Michigan



Background

Chlorine Chemistry in the Arctic

- In the atmosphere, chlorine species (e.g. Cl₂) can undergo photolysis, producing chlorine radicals (•Cl), which significantly speed up the oxidation of atmospheric compounds such as the greenhouse gas methane¹⁻³

Figure 1: Overview of Arctic chlorine chemistry.

Goals of this work

- investigate atmospheric chlorine chemistry, including the production of Cl radicals using measurements of Cl₂, BrCl, & ClNO₂
- Explore the potential effect of nitrogen oxides (NO_x = •NO + •NO₂) and subsequently nitryl chloride (ClNO₂) on the Cl budget
 - ClNO₂ is a halogenated derivative of nitrogen oxides commonly measured in polluted coastal areas in the mid-latitudes⁵. Serves as a reservoir species for •Cl and •NO₂¹
 - Currently no published observations of ClNO₂ in the Arctic

Observations of Episodic Chlorine Chemistry

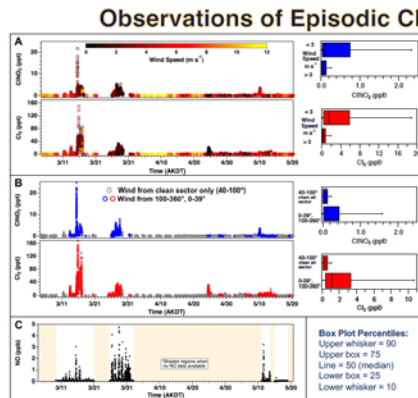


Figure 3: Time series of Cl₂ (A) and ClNO₂ (B), colored by wind speed and direction. Box plots compare Cl₂ and ClNO₂ during different wind speed and direction conditions. The "clean air sector" is at 40-100°. Concurrent Cl₂ and NO measurements are also shown when data were available (C).

Figure 4 (right): Wind rose for the entire study period (3/4-5/20). "Clean air sector" is 40-100° (between blue lines). The prevailing NE-E winds dominated, but occasionally winds came from polluted sectors and were of lower speeds.

Methods

Ambient sampling was conducted at a coastal tundra field site SE of Utqiagvik (Barrow), AK from Mar 4 – May 20, 2016

Chemical ionization mass spectrometry (CIMS) was used to continuously monitor Cl₂, ClNO₂, & BrCl using iodide adduct formation, with I(H₂O)₂ as the reagent ion.¹⁰

- 3σ LODs:** Cl₂: 0.8 ppt; ClNO₂: 0.3 ppt; BrCl: 2.5 ppt
- Calibration:** Cl₂ was routinely calibrated using a permeation device (VICI), and ClNO₂ was synthesized via Cl₂ + NO₂, and quantified by thermal dissociation to NO₂.¹¹ BrCl calibration factor was estimated as the average of Cl₂ and Br₂ sensitivities.¹²

Nitrogen oxides (NO_x=NO+NO₂) were measured by a Model 42i Thermo Scientific NO_x analyzer via chemiluminescence. LOD: 0.4 ppb

Wind speed and direction were measured by a propeller anemometer attached to a co-located 11.5 m tall tower

- Periods of missing data (3/4 – 3/17) were supplemented by the nearby NOAA ESRL/GMD Barrow Observatory

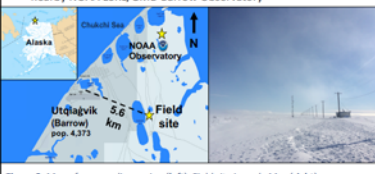


Figure 2: Map of surrounding region (left); Field site in early May (right).

Effect on Chlorine Atom Production Rate

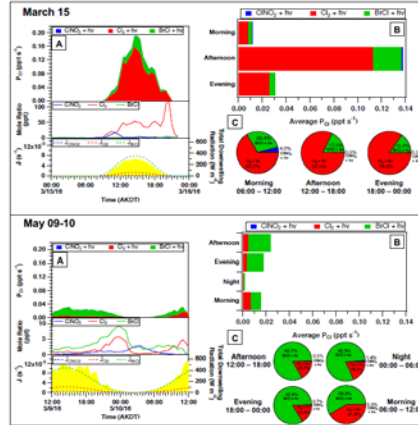


Figure 5: Photolysis of ClNO₂, Cl₂, and BrCl as a source for Cl atoms (Figure 5 left):

- CIMS measurements and calculated photolysis frequencies were used to determine the chlorine atom production (P_{Cl}) budget during active chlorine chemistry on **Mar 15** (top panel) and **May 09-10** (bottom panel)
- Figure 5A: Time series of P_{Cl} by Cl atom source, measured Cl atom precursors (ClNO₂, Cl₂, & BrCl), and calculated photolysis frequencies & observed solar radiation
- Figure 5B: Average P_{Cl} magnitude during selected 6 h periods
- Figure 5C: Relative contribution of each Cl atom source to total P_{Cl} during selected 6 h periods

Main points:

- Overall P_{Cl} was "6x faster on Mar 15 than in mid-May. This is likely due to ~10x more Cl₂ observed on this day than in May (40-60 ppt in the afternoon) leading to faster photolysis.
- P_{Cl} was dominated by the photolysis of Cl₂ on Mar 15 (66-85%). However, BrCl photolysis dominated P_{Cl} on May 09-10, contributing 58-83%.
- ClNO₂ photolysis was not a major contributor to the overall P_{Cl} in Mar and in May. Photolysis of ClNO₂ contributed up to 4% of P_{Cl} in the morning of Mar 15 and 1.4% during the night of May 10.

References

- Simpson, W. R. et al. Chem. Rev. 2015, 115, 4023-4062.
- Young et al. Atmos. Chem. Phys. 2014, 14, 3427-3440.
- Coatard et al. Earth Space Chem. 2017, 1, 17.
- Impre, G. A. et al. J. Geophys. Res. 1997, 102 (D13), 15999-16004.
- Liao, J. et al. Nat. Geosci. 2014, 7(2), 91-94, 13169-13180.
- Stephens et al. J. Geophys. Res. Atmos. 2012, 117, D00R11
- Spicer et al. Atmos. Environ. 2002, 36, 2721-2731.
- Cutshall et al. Nat. Geosci. 2008, 1, 324-328.
- Liao, J. et al. J. Geophys. Res. 2011, 116, D08R02.
- Thaler et al. Anal. Chem. 2011, 83, 2763-2766.
- Arbaugh et al. J. Phys. Chem. A. 2012, 116, 6527-6533.
- Khorram et al. Geophys. Res. Lett. 1999, 26(6), 659-668.
- Simpson et al. Geophys. Res. Lett. 2005, 32(4), 1-4.
- Custard et al. Environ. Sci. Technol. 2016, 50, 12394-12400.

Key Findings and Implications

- We report the first measurements of ClNO₂ of up to 24 ppt, in the Arctic. Up to 150 ppt of Cl₂ was also observed, consistent with previous Barrow observations by Liao et al.⁹ and Custard et al.¹³
- The highest Cl₂ and ClNO₂ mixing ratios were observed when high NO was present. These episodes were characterized by low wind speeds (< 3 m s⁻¹) from the polluted sector
- Measurements of three Cl atom precursors, ClNO₂, Cl₂, and BrCl, and calculated photolysis frequencies were used to determine chlorine atom production rates (P_{Cl}) for selected episodes of active halogen chemistry:
 - Cl₂ and BrCl photolysis were by far the largest contributors to the overall P_{Cl} on these days.
 - Photolysis of ClNO₂ contributed at most 4% to the overall P_{Cl} (morning of Mar 15)

In the future

- Despite ClNO₂'s minimal contribution to the Cl atom production rate, its role is expected to grow as shipping and fossil fuel extraction continue to expand in the Arctic, potentially bringing more NO_x emissions
- Snowpack sampling and flux studies are needed to further understand ClNO₂ and BrCl production in the Arctic

Acknowledgments

Funding: NSF Grants PLR-1417668, PLR-1417906, PLR-1417914, UM Rackham Graduate School. We thank NOAA Earth System Research Laboratory, Global Monitoring Division Barrow for wind data, Kathryn Koleas for assistance with calibrations, and UIC Science, Polar Field Services, Jesus Ruiz-Piñancarte and Dandan Wei for logistical support.

Winner

Emma Mungall

(U Toronto)

UNIVERSITY OF TORONTO

A novel source of oxygenated volatile organic compounds in the summer time marine Arctic boundary layer

EMNETCARE

Emma L. Mungall¹, Jonathan P. D. Abbott¹, Jeremy J. B. Wentzell², Alex K. Y. Lee³, Jennie L. Thomas⁴, Marjolaine Blais⁵, Michel Gosselin⁶, Lisa Miller⁶, Tim Papakyriakou⁷, and John Liggit⁸

¹Department of Chemistry, University of Toronto ²Environment Canada ³National University of Singapore ⁴LATMOS, Paris ⁵Université de Québec à Rimouski ⁶Fisheries and Oceans Canada ⁷University of Manitoba

1. Introduction & Hypothesis

- OVOCs can contribute to new particle formation¹ and to the growth of aerosol particles in the atmosphere² through the formation of secondary organic aerosol (SOA), which can affect climate directly by scattering radiation and indirectly by influencing cloud formation and properties
- Few measurements have been made of OVOCs in the remote marine boundary layer; some researchers have concluded that known sources can't account for measured values^{3,4}
- A possible candidate for this missing source was identified by recent lab work^{5,6,7,8} elucidating a new mechanism of OVOC formation from the sea surface microlayer (SML) (shown below)
- We present the first ambient observations of OVOCs produced by this mechanism

Fig. 1. a) Polar projected map showing the Central Arctic Ocean, the Canadian Archipelago and Northern Greenland. The land type data are taken from the Olson Land Map¹¹ and the sea ice data is from the NSIDC¹² for 1 August, 2016. The yellow star highlights the location (Nares Strait) where we observed the maximum oceanic source of OVOCs. b) A schematic of the proposed OVOC generation mechanisms (A: photochemical, B: dark ozonolysis) at the study site.

2a. Experimental Methods

Data were collected during Leg 1 of the CGCS Amundsen cruise in 2014 as part of the EMNETCARE project.

Species	Instrument	Details
OVOCs	Acetate CIMS	Sampled from the bridge; online high resolution method
DMS, isoprene	Benzene CIMS	Sampled from tower at the bow; online high resolution method
DOC	Shimadzu TOC-VCPN	Collected from 2.5 m depth with a rosette sampler equipped with 12 L Niskin bottles
CDOM	Variable ECO-CDOM fluorometer	Mounted on the rosette
Incoming short wave solar radiation flux	pyranometer (Q285-2.8, Espy) FSR60	Mounted ~20 m above sea level

2b. Data Analysis Methods

Positive matrix factorization (PMF) analysis yielded a 4-factor solution, of which one factor is presented here.

Time series of the most intense calibrated components of this factor are shown at far left.

3. Results & Discussion

Evidence for SML mechanism

- Correlation between DOC and PMF Ocean Factor
- Correlation between Ocean Factor and CDOM ($R^2 = 0.42$)
- Correlation between diurnal cycles of solar radiation and PMF Ocean Factor ($R^2 = 0.45$)

Local, marine-influenced air mass

- FLEXPART-WRF backward runs show local marine influence at this time
- Concurrent studies concluded little long-range transport
- Correlations between long- and short-lived species indicate common local source ($R^2 = 0.58$ for formic and levulinic acids)
- Other OVOC sources unlikely in the region (little ground-level snow in July & August, sparse vegetation at extremely high latitudes)

Evidence against wind-driven flux

- No correlation with insoluble ocean-emitted compounds DMS and isoprene (at left, $R^2 < 0.1$)
- box-model using MCMv3.2 and Atochem could not account for measured formic acid
- Calculations of necessary aqueous concentrations of measured acids far exceed measured DOC pool

2a. Experimental Methods

Data were collected during Leg 1 of the CGCS Amundsen cruise in 2014 as part of the EMNETCARE project.

Species	Instrument	Details
OVOCs	Acetate CIMS	Sampled from the bridge; online high resolution method
DMS, isoprene	Benzene CIMS	Sampled from tower at the bow; online high resolution method
DOC	Shimadzu TOC-VCPN	Collected from 2.5 m depth with a rosette sampler equipped with 12 L Niskin bottles
CDOM	Variable ECO-CDOM fluorometer	Mounted on the rosette
Incoming short wave solar radiation flux	pyranometer (Q285-2.8, Espy) FSR60	Mounted ~20 m above sea level

2b. Data Analysis Methods

Positive matrix factorization (PMF) analysis yielded a 4-factor solution, of which one factor is presented here.

Time series of the most intense calibrated components of this factor are shown at far left.

4. Implications & Conclusion

- Many of the Ocean Factor molecules are classified as OVOCs & SVOCs¹⁴ and thus have the potential to contribute to SOA formation¹⁴
- Small organic acids can participate in aqueous oligomerization reactions¹⁵ High RH and frequent fog in the summer Arctic make this a possible path to SOA formation
- We suggest that this source may be widespread and could be important to our understanding of secondary organic aerosol in remote marine environments, with implications for our understanding of global climate.

5. References

1. Zhang, H. et al. (2014) Nature 512, 453-456. 2. Tegen, I. et al. (2015) Nature 521, 529-532. 3. Berman, D. et al. (2014) Atmos. Chem. Phys. 14, 1081-1090. 4. Gosselin, M. et al. (2014) Atmos. Chem. Phys. 14, 1081-1090. 5. Mungall, E. L. et al. (2014) Atmos. Chem. Phys. 14, 1081-1090. 6. Mungall, E. L. et al. (2014) Atmos. Chem. Phys. 14, 1081-1090. 7. Mungall, E. L. et al. (2014) Atmos. Chem. Phys. 14, 1081-1090. 8. Mungall, E. L. et al. (2014) Atmos. Chem. Phys. 14, 1081-1090. 9. Mungall, E. L. et al. (2014) Atmos. Chem. Phys. 14, 1081-1090. 10. Mungall, E. L. et al. (2014) Atmos. Chem. Phys. 14, 1081-1090. 11. Olson, J. et al. (2003) J. Geophys. Res. 108, 4102. 12. NSIDC. 13. Mungall, E. L. et al. (2014) Atmos. Chem. Phys. 14, 1081-1090. 14. Mungall, E. L. et al. (2014) Atmos. Chem. Phys. 14, 1081-1090. 15. Mungall, E. L. et al. (2014) Atmos. Chem. Phys. 14, 1081-1090.

6. Acknowledgements

We are grateful for the support of the officers, crew and scientists aboard the Amundsen in 2014. ArcticNet, and specifically Keith Lawrence, Maurice Lévesque and Jennifer Murphy for their support and facilitating data collection during the cruise. We wish to acknowledge Tom Burgess for help with the meteorological data and Vicki Irish and Marine Lussier for sea-surface microlayer samples. Tom Burgess and Marjolaine Blais provided helpful discussions concerning the use of the benzene reagent ion, and discussions with Marjolaine clarified our understanding of the Arctic Ocean circulation. FLEXPART-WRF computer modeling benefited from access to GRC/HPC resources (OVOC allocations 2015-01741 and 2016-01741) and the PPL mesoscale computing center (SOA4D; Centur Internet portal in Canada; 100megapb at U. de Sherbrooke). We thank Samuel Meunier for introducing us to using MCMv3.2 in Atochem and Environment and Climate Change Canada for their support. We would like to thank Claude Rivest for DOC analysis. This campaign was done under the EMNETCARE project which is an EMNETCARE funded program.

A novel source of oxygenated volatile organic compounds in the summertime marine Arctic boundary layer

PDF Winner (1)

Winner

Peter Peterson

(U Michigan)

Airborne Imaging of Bromine Monoxide Over Northern Alaska With Differential Optical Absorption Spectroscopy (DOAS)



Airborne Imaging of Bromine Monoxide Over Northern Alaska With Differential Optical Absorption Spectroscopy (DOAS)

Peter Peterson^{1*}, William Simpson², Son Nghiem³, Johannes Zielcke⁴, Stephan General⁴, Denis Pöhler⁴, Udo Frieß⁴, Ulrich Platt⁴, Paul Shepson⁵, Holger Sihler⁶, and Kerri Pratt¹

¹Department of Chemistry, University of Michigan

²Department of Chemistry and Biochemistry and Geophysical Institute, University of Alaska Fairbanks

³Jet Propulsion Laboratory, California Institute of Technology

⁴Institute of Environmental Physics, University of Heidelberg, Germany

⁵Department of Chemistry and Earth, Planetary, and Atmospheric Sciences, Purdue University

⁶Max Planck Institute for Chemistry, Mainz, Germany



BACKGROUND AND KEY QUESTIONS

- Polar sunrise in the Arctic is associated with reactive halogen (e.g. Br, BrO) production linked to O₃ depletion and Hg deposition (Simpson et al 2007)
- Environmental parameters influencing BrO_x production are not fully understood, and likely influenced by rapidly changing Arctic environment
- Satellites measure BrO across the Arctic, but with low spatial resolution and limited ability to examine the vertical distribution of BrO, while ground-based MAX-DOAS is usually fixed in one location and has limited vertical resolution
- To understand impacts of this chemistry, knowledge of the spatial distribution of BrO, both horizontally and vertically, is required and currently lacking
- Airborne imaging DOAS is uniquely suited to simultaneously profile the vertical and horizontal distributions of BrO with high spatial resolution over a large region

2012 BROMINE OZONE & MERCURY EXPERIMENT



Fig. 1: Location of the BROMEX campaign

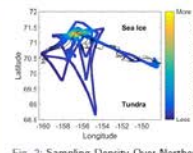


Fig. 2: Sampling Density Over Northern Alaska

- The 2012 Bromine, Ozone, and Mercury Experiment (BROMEX) involved satellite, airborne, and ground-based observations of the cryosphere and atmospheric composition during March and April (Nghiem et al 2012)
- This interdisciplinary project aimed to investigate impacts of Arctic sea ice reductions on bromine, ozone, and mercury in the atmosphere
- As part of the BROMEX campaign, 9 flights of the Purdue University Airborne Laboratory for Atmospheric Research (ALAR) were conducted around the vicinity of Utqiagvik, Alaska, between Mar. 13 and Mar 31st, to explore halogen activation processes throughout the region
- ALAR equipped with the Heidelberg Airborne Imaging DOAS instrument (HAIDI) (General et al 2014)
- Other instruments on-board ALAR enabled in-situ measurements of O₃, meteorology, aerosol particle number concentrations, and aerosol particle size distributions

HEIDELBERG AIRBORNE IMAGING DOAS INSTRUMENT

- Differential Optical Absorption Spectroscopy (DOAS) allows for retrieval of information about BrO distributions using measurements of solar spectra
- HAIDI equipped with two DOAS instruments, one nadir and one limb viewing
- Nadir viewing instrument allows mapping of BrO lower tropospheric vertical column densities (LT-VCDs) at 100 m spatial resolution, an improvement on satellite based measurements (10s of km)
- HAIDI's forward imaging telescope observes spectra over a 7 degree range in front of the aircraft (+2° to -5° relative to horizon)
- HAIDI builds on conventional limb viewing measurements allowing continuous profiling of BrO

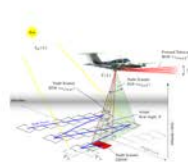


Fig. 3: Viewing geometry for HAIDI showing both the nadir view and the limb view. Figure from General et al 2014

OBSERVATIONS OF REACTIVE BROMINE TRANSPORT ALOFT

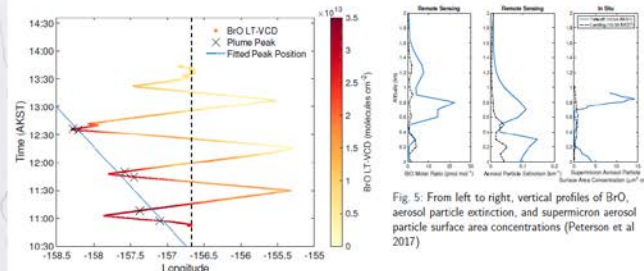


Fig. 4: BrO LT-VCDs plotted as a function of longitude and time from the Mar 13 flight. The peak LT-VCD is plotted as a black X. The linear fit shows the westward motion of the plume at a speed consistent with that of the airmass (8 m/s)

- Plane flew east-west transects in and out of a reactive bromine plume as it moved west
- Vertical profiles at takeoff and landing showed BrO mixing ratios as high as 20 pmol mol⁻¹ at 750 m aloft, coincident with enhancements in supermicron aerosol particles
- These observations show supermicron particles aloft enable the transport of reactive bromine disconnected from the snowpack (Peterson et al 2017)

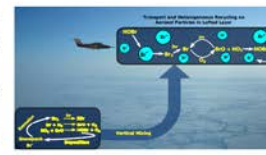


Fig. 5: From left to right, vertical profiles of BrO, aerosol particle extraction, and supermicron aerosol particle surface area concentrations (Peterson et al 2017)

SNOWPACK DRIVEN BR O PRODUCTION 200 KM INLAND

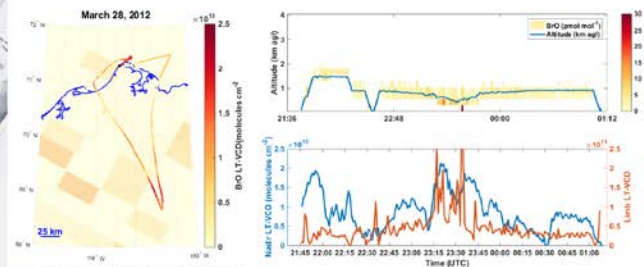


Fig. 7: Flight track colored by BrO LT-VCD and overlaid on LT-VCD data derived from GOME-2 satellite measurements (Sihler et al 2012)

Fig. 8: Top) Limb viewing measurements of BrO mixing ratios. Bottom) Comparison of LT-VCDs derived from limb and nadir viewing measurements

- Limb measurements have limited near surface sensitivity at higher altitudes and when plane is undergoing altitude changes
- Limb LT-VCDs are typically lower than nadir LT-VCDs, indicating BrO at the surface
- Enhancements in near surface BrO 200km inland indicate tundra snowpack driven halogen activation far from sea ice regions

CONCLUSIONS

- These remote sensing measurements allow retrieval of trace gas vertical profile and total column information without variation in aircraft altitude enabling high resolution 3-D mapping
- Supermicron particles aloft enable transport of reactive bromine aloft, decoupled from the snowpack
- Inland snowpacks drive bromine activation, extending impacts of halogen chemistry beyond sea ice regions

ACKNOWLEDGMENTS AND REFERENCES

Financial support for this work was provided by the National Aeronautics and Space Administration (NASA) Earth Science Research Program (NNSA18PAC). Funding for the airborne measurements was provided by NASA's Constellation Science Program as a part of the NASA Interdisciplinary Research on Arctic Sea Ice and Tropospheric Chemical Change (IS-2009-31). The research carried out at the Jet Propulsion Laboratory, California Institute of Technology, was supported by the NASA Constellation Science Program. The development and operation of the HAIDI instrument was funded by the Deutsche Forschungsgemeinschaft (DFG) within the Priority Program (SPP) No. 1298 "HALO" (DFG: PE-384/1-1 and 1/2). GOME-2 level 1 data were provided by EUMETSAT.

- Simpson et al 2007, ACP
- Nghiem et al 2012, EOS
- General et al 2014, AMT
- Peterson et al 2017, ACP
- Sihler et al 2012, ACP

Thank you to our judges:

Judges for PhD and PDF posters:

Lukas Arenson
Claude Duguay
Alexandra Jahn
Kent Moore
Kerri Pratt

Judges for MSc posters:

Session A:

Roghayeh (Roya) Ghahremaninezhad
Thomas Oudar

Session B:

Yukari Hori
Peter Peterson